

SOLVING THE MILD-SLOPE AND HELMHOLTZ EQUATIONS USING THE VIRTUAL ELEMENT METHOD (VEM), DEALING WITH HIGH ORDER ROBIN BOUNDARY CONDITION

R. Dupont^{1,2} and M. Dauphin³, R. Mottier^{4,5,6}

July 22, 2024

¹ GEOSCIENCES-M, Univ Montpellier, CNRS, Montpellier, France.

² IMAG, Univ Montpellier, CNRS, Montpellier, France.

³ Scuola Superiore Meridionale, Napoli, Italy.

⁴ École nationale des ponts et chaussées, France.

⁵ Commissariat à l'énergie atomique et aux énergies alternatives, France.

⁶ Institut national de recherche en sciences et technologies du numérique, France.

*Corresponding authors. E-mail(s): ronan.dupont@umontpellier.fr;
mathias.dauphin-ssm@unina.it; romain.mottier@outlook.com.

Abstract

The numerical solution of the Mild-slope equation (MSE) is crucial in various fields, including coastal engineering, oceanography, and offshore structure design. In this article, we present a novel approach utilizing the Virtual Element Method (VEM) for the numerical solution of the MSE. The VEM offers significant advantages over traditional finite element methods, particularly in handling complex geometries and irregular meshes. We first look at the implementation and validation of the model in the presence of Robin boundary conditions. We then apply the results to the calculation of eigenmodes for the port of Cherbourg.

Keywords. Mild-slope equation, Helmholtz equation, Virtual Element Method, computational fluid dynamics, validation, Finite Element Methods, Numerical Analysis, Complex Geometries, Irregular Meshes, Robin Boundary Condition, Coastal Engineering.

Contents

1	Introduction	3
2	Model Problem	4
3	Solving Equations Using the Virtual Element Method	5
3.1	Variational formulation	5
3.1.1	The Helmholtz Equation	5
3.1.2	The Mild-Slope Equation	6
3.2	Dofs	7
3.3	Robin Boundary Condition	9
3.4	Numerical Validation	11
4	Numerical Application	12
4.1	Sensibilité de la pente, Helmholtz vs Berkhoff	12
4.2	Application claquée - Résultats avec différents k	13
4.3	Sensibilité du coefficient de réflexion	14
4.4	Appli montrant intérêt Robin	15
5	Conclusion and Discussion	16
6	Declarations	17
6.1	Availability of data and material	17
6.2	Conflict of interest	17
6.3	Acknowledgements	17
A	Manufactured analytical solution	17

1 Introduction

Nowadays, coastal modeling has become a major challenge in the face of climate change. Coastal-related topics have become very numerous, including ocean modeling (large-scale), port modeling and numerous other topics such as morphodynamics. In this study, we are particularly interested in port modeling through the equation models developed by Helmholtz (1868) and Berkhoff (1972). These two equation models can be used in coastal modeling to calculate wave agitation inside a harbor. The Helmholtz (1868) equation is a very classical equation, which can be used in various fields such as electromagnetics or acoustics. In our study, it is used for flat sea bottoms, while the Berkhoff (1972) equation, also known as the Mild-Slope equation, is used for variable bottoms with a maximum slope of 1/3 (Booij 1983). In this study, we have chosen to solve these equations using the virtual element method (Beirão da Veiga et al. 2014) MATHIAS, tu peux ajouter qqls autres refs importantes stp. This method has the advantage of i) being a high-order finite element method, which enables wave phenomena to be accurately captured, where simple finite elements have difficulty capturing them RORO, tu peux ajouter des références pour ce que tu disais, que sur des méthodes FEM simple, même en raffinement, on arrivait pas à capturer tous les phénomènes ondulatoires., ii) handle polyhedral meshes as well as non-conforming meshes, enabling simple refinement in certain areas. Although a few studies have already dealt with the Helmholtz (1868) problem in virtual elements (Perugia et al. 2016; Mascotto et al. 2019), none of them has had any concrete application in the coastal sector. In this study, we will first express the modeling of the problem. Next, we will explain the virtual element strategy for approximating this problem. Finally, we'll look at a particular boundary condition, the Robin condition. After validating our model, we will apply it to the calculation of eigenvalues for the port of Cherbourg.

Vous pouvez étoffer un peu, c'est un draft.

2 Model Problem

In this section, we consider the wave problem described in figure 1.

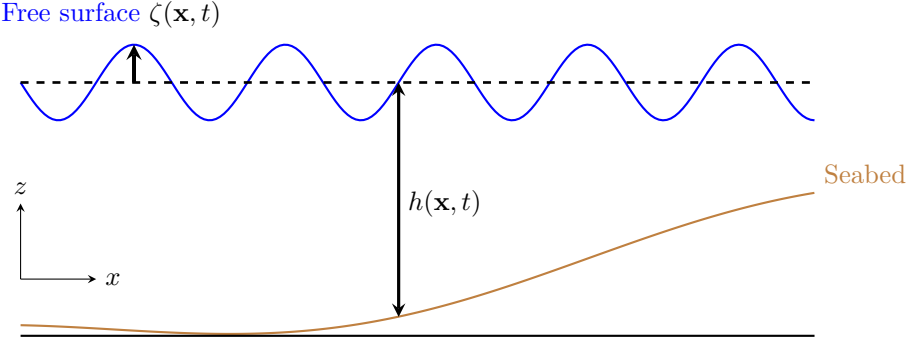


Figure 1: Sketch of a free surface elevation ζ in the (x, z) -plane.

with ζ the free surface defined by $\zeta(\mathbf{x}, t) = \Re\{\eta(x, y) e^{-i\omega t}\}$, η a complex-valued amplitude of ζ , $\omega = 2\pi/T_0$ the angular frequency, T_0 the wave period and h the depth.

The amplitude η can be split into its incident and reflective part,

$$\eta = \eta_I + \eta_R.$$

We thus have,

$$\eta_I(\mathbf{x}, t) = a_I(\mathbf{x})e^{-i\omega t} \quad \text{and} \quad \eta_R(\mathbf{x}, t) = a_R(\mathbf{x})e^{-i\omega t}$$

with the incident wave amplitude defined by,

$$a_I(\mathbf{x}) = a_{\max} e^{-i\mathbf{k}\mathbf{x}} \quad \text{with} \quad \mathbf{k} = k(\cos(\theta), \sin(\theta))^T,$$

with θ the incident wave angle, a_{\max} the maximum wave amplitude.

The amplitude of the reflected wave a_R is obtained by solving the Helmholtz (1868) equation, in the case of a flat bottom,

$$\begin{cases} \Delta a + k^2 a = 0, & \text{in } \Omega, \\ a = a_I, & \text{in } \Gamma_{\text{in}}, \\ \frac{\partial a}{\partial n} + ik a = 0, & \text{in } \Gamma_{\text{out}}, \\ a = -\gamma a_I & \text{in } \Gamma_D. \end{cases} \quad (1)$$

with $\gamma \in [0, 1]$ the reflection coefficient, k the wave number: solution of the dispersion relation at order 1 (equation (2)) from linear theory (Airy 1845),

$$\omega^2 = g k \tanh(kh) \quad \text{with} \quad \omega = \frac{2\pi}{T_0}. \quad (2)$$

The amplitude of the reflected wave a_R can also be obtained by solving the Mild-Slope equation (Berkhoff 1972), in the case of a variable bottom,

$$\left\{ \begin{array}{ll} \nabla(C_p C_g \nabla a) + k^2 C_p C_g a = 0, & \text{in } \Omega, \\ a = a_I, & \text{in } \Gamma_{\text{in}}, \\ \frac{\partial a}{\partial n} + ik a = 0, & \text{in } \Gamma_{\text{out}}, \\ a = -\gamma a_I & \text{in } \Gamma_{\text{D}}. \end{array} \right. \quad (3)$$

with

$$C_p = \frac{\omega}{k} \quad \text{and} \quad C_g = \frac{1}{2} C_p \left[1 + kh \frac{1 - \tanh^2(kh)}{\tanh(kh)} \right]. \quad (4)$$

The choice of boundary conditions will be explained in the application section 4.

Remarks:

- In practice, k is obtained simply by using the Guo (2002) approximation.
- Assuming constant depth within the port and $C_g = C_p/2$ (as in shallow water) and noting that $C_p = \omega/k = Cte$, equation (3) can be simplified to yield the Helmholtz (1868) equation.

3 Solving Equations Using the Virtual Element Method

In this section, we develop the variational formulation of the problem and briefly recall the formalism of virtual elements to solve the problem.

Eventuellement à completer.

3.1 Variational formulation

We decompose this subsection into two parts, one expressing the variational formulation for the Helmholtz (1868) equation (1) and another for that of the Mild-Slope equation (3).

3.1.1 The Helmholtz Equation

We consider the Helmholtz (1868) equation (1) and thus the following variational formulation:

$$\left\{ \begin{array}{l} \text{find } u \in V = H_0^1(\Omega) \text{ such that} \\ a(u, v) = 0 \quad \forall v \in V, \end{array} \right. \quad (5)$$

where,

$$\begin{aligned} a(u, v) &= \int_{\Omega} \Delta u v + k^2 \int_{\Omega} u v + k^2 \int_{\Gamma_{\text{out}}} \frac{\partial u}{\partial n} v \\ &= \int_{\Omega} \Delta u v + k^2 \int_{\Omega} u v - ik \int_{\Gamma_{\text{out}}} u v \end{aligned} \quad . \quad (6)$$

We build a discrete problem in following form:

$$\begin{cases} \text{find } u_h \in V_h \subset V \text{ such that} \\ a(u_h, v_h) = 0 \quad \forall v \in V, \end{cases} \quad (7)$$

where $V_h \subset V$ is a finite dimensional space and $a_h(\cdot, \cdot) : V_h \times V_h \rightarrow \mathbb{R}$ is a discrete bilinear form approximating the continuous form $a(\cdot, \cdot)$.

We thus have the discrete form:

$$\begin{aligned} a_h(u_h, v_h) &= \sum_{E \in \Omega_h} \left[\int_E \Delta u_h v_h + \int_E k^2 u_h v_h \right], \\ &\stackrel{\substack{\text{green} \\ \partial u / \partial n = -ik u}}{=} \sum_{E \in \Omega_h} \left[- \int_E \nabla u_h \nabla v_h + \int_E u_h v_h - \mathbb{1}_{\Gamma_{\text{out}} \subset E} i \int_{\Gamma_{\text{out}}} k u_h v_h \right]. \end{aligned} \quad (8)$$

with $\mathbb{1}_{\Gamma_{\text{out}} \subset E}$ the indicator function and $u = u + u_D$ and u_D is the lifting of $-\gamma a_I$ or a_I (depending on the border).

3.1.2 The Mild-Slope Equation

Now, we consider the [Berkhoff \(1972\)](#) equation (3) and thus the following variational formulation:

$$\begin{cases} \text{find } u \in V = H_0^1(\Omega) \text{ such that} \\ a(u, v) = 0 \quad \forall v \in V, \end{cases} \quad (9)$$

where,

$$a(u, v) = \int_{\Omega} \nabla(C_p C_g \nabla u v) + \int_{\Omega} k^2 C_p C_g u v \quad . \quad (10)$$

We build a discrete problem in following form:

$$\begin{cases} \text{find } u_h \in V_h \subset V \text{ such that} \\ a(u_h, v_h) = 0 \quad \forall v \in V, \end{cases} \quad (11)$$

where $V_h \subset V$ is a finite dimensional space and $a_h(\cdot, \cdot) : V_h \times V_h \rightarrow \mathbb{R}$ is a discrete bilinear form approximating the continuous form $a(\cdot, \cdot)$.

We thus have the discrete form:

$$\begin{aligned}
a_h(u_h, v_h) &= \sum_{E \in \Omega_h} \left[\int_E \nabla(C_p C_g \nabla u_h v_h) + \int_E k^2 C_p C_g u_h v_h \right], \\
&\stackrel{1/E \int_E C_p C_g = \mathcal{A}_E}{\approx} \sum_{E \in \Omega_h} \left[\mathcal{A}_E \int_E (\Delta u_h v_h) + \mathcal{B}_E \int_E u_h v_h \right], \\
&\stackrel{\partial u / \partial n = -ik u}{=} \sum_{E \in \Omega_h} \left[-\mathcal{A}_E \int_E \nabla u_h \nabla v_h + \mathcal{B}_E \int_E u_h v_h - \mathbb{1}_{\Gamma_{\text{out}} \subset E} i \mathcal{A}_E \int_{\Gamma_{\text{out}}} k u_h v_h \right].
\end{aligned} \tag{12}$$

with $\mathbb{1}_{\Gamma_{\text{out}} \subset E}$ the indicator function and $u = u + u_D$ and u_D is the lifting of $-\gamma a_I$ or a_I (depending on the border).

Remark: Unlike the discrete formulation of the homogeneous Helmholtz (1868) equation (8), the discrete formulation of the Mild-Slope equation (12) assumes that k^2 and $C_p C_g$ are constant for each cell in the mesh.

3.2 Dofs

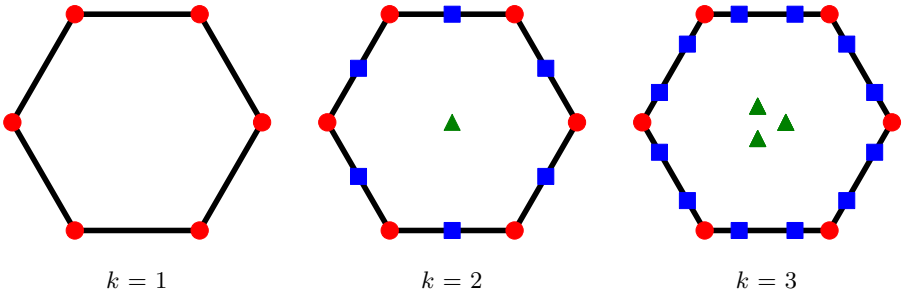


Figure 2: 2D element with ● : Summits dofs, ■ : Edges dofs, ▲ : Inner dofs.

Let Ω_h be a simple polygonal mesh on Ω . This can be any decomposition of Ω in non overlapping polygons E with straight faces. The space V_h will be defined element-wise, by introducing

- local spaces $V_{h|E}$;
- the associated local degrees of freedom.

For all $E \in \Omega_h$:

$$\begin{aligned}
V_{h|E} &= \left\{ v_h \in H_0^1(\Omega) \cap C^0(\partial E) : v_h|_{\partial E} \in \mathbb{P}_k(E), \Delta v_h \in \mathbb{P}_k(E) \right. \\
&\quad \left. (\Pi_k^\nabla v_h - v_h, p)_{0,E} = 0, \forall p \in \mathbb{P}_k(E)/\mathbb{P}_{k-2}(E) \right\}
\end{aligned} \tag{13}$$

where $\mathbb{P}_k(E)/P_{k-2}(E)$ is the subspace of $\mathbb{P}_k(E)$ of the polynomials that are orthogonal in the sense of L^2 to $\mathbb{P}_{k-2}(E)$, or, alternatively, the polynomials of degree $k - 1$ and k .

- the functions $V_{h|E}$ are continuous (and known) on ∂E ;
- the functions $V_{h|E}$ are unknown on E !
-

1. Mesh Decomposition: We consider a polytopal decomposition $\{T_h\}_h$ of the domain Ω which is regular—that is, there exists $\rho \in (0, 1)$, independent of h , such that every element $E \in T_h$ is star-shaped with respect to a ball of radius $\geq \rho h_E$, with h_E the diameter of E .

2. Local Projections: We denote by $\Pi_k^{\nabla, E} : H^1(E) \rightarrow \mathbb{P}_k(E)$ and $\Pi_k^{0, E} : L^2(E) \rightarrow \mathbb{P}_k(E)$ the usual lo elliptic projection and local L^2 -projection respectively onto the space of polynomials of degree a most k .

3. Virtual Space: We define the local virtual space by

$$V_h^E = \left\{ v_h \in H_0^1(\Omega) \cap C^0(\partial E) : v_h|_{\partial E} \in \mathbb{P}_k(E), \Delta v_h \in \mathbb{P}_k(E) \right. \\ \left. (\Pi_k^\nabla v_h - v_h, p)_{0, E} = 0, \forall p \in \mathbb{P}_k(E)/\mathbb{P}_{k-2}(E) \right\}$$

where $\mathbb{P}_k(E)/\mathbb{P}_{k-2}(E)$ is the subspace of $\mathbb{P}_k(E)$ of the polynomials that are orthogonal in the sense of L^2 to $\mathbb{P}_{k-2}(E)$, or, alternatively, the polynomials of degree $k-1$ and k .

3. DDL

4. Base:

$$m_{\alpha_1, \alpha_2} = \left(\frac{x - x_D}{h_D} \right)^{\alpha_1} \cdot \left(\frac{y - y_D}{h_D} \right)^{\alpha_2}$$

Soit $V = \{v \in H^1(\Omega), v|_{\Gamma_D} = 0\}$.

$$\int_{\Omega} \Delta u v + \int_{\Omega} k^2 u v = 0, \quad \forall v \in V.$$

En appliquant la formule de Green, on a :

$$-\int_{\Omega} \nabla u \nabla v + \int_{\Gamma_{Inf}} \frac{\partial u}{\partial n} v + k^2 \int_{\Omega} u v = 0, \quad \forall v \in V.$$

$$-\int_{\Omega} \nabla u \nabla v - ik \int_{\Gamma_{Inf}} u v + k^2 \int_{\Omega} u v = 0, \quad \forall v \in V.$$

3.3 Robin Boundary Condition

Nous allons construire la matrice $B = (\int_{\partial\Omega} \alpha(\Phi_j(x, y), \Phi_i(x, y))_{i,j})$ en parcourant les éléments frontières du bord. Ces éléments sont des segments joignant 2 points consécutifs du bord. La fonction de base Φ_i attachée au sommet i du bord, restreinte à l'élément de bord est une fonction \mathbb{P}_k du bord.

Les éléments du bord sont de longueur $\lambda(e)$. Pour un élément de référence de la forme $[\xi_0, \xi_0 + \lambda]$ entre deux points V_0 et V_1 .

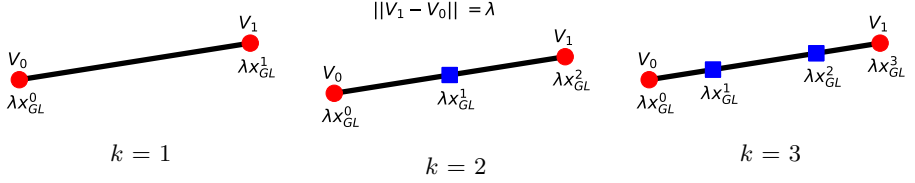


Figure 3: 1D element $[\xi_0, \xi_0 + \lambda]$ representation with ● : Summits dofs, ■ : Edges dofs.

La matrice élémentaire associée à ce terme de Robin est de la forme

$$elb = \left(\int_0^\lambda \alpha_*(\xi_0 + \xi) \varphi_j(\xi) \varphi_i(\xi) d\xi \right)_{1 \leq i, j \leq k+1}, \quad (14)$$

avec $\alpha_*(\xi_0 + \xi) = \alpha(V_0|_x + \xi t_x, V_0|_y + \xi t_y)$ et \vec{t} est le vecteur unitaire orienté de V_0 à V_1 . Pour $i, j \in \llbracket 0, k \rrbracket$:

$$\varphi_i(\lambda x_{GL}^j) = \delta_j^i,$$

avec x_{GL}^j le $j - i$ eme point de quadrature de Gauss-Lobatto sur $[0, 1]$. On trouve les φ_i aisément avec les polynômes de Lagrange comme suivant:

$$\begin{aligned} \varphi_i(\xi) &= \sum_{j=0}^k \delta_j^i \left(\prod_{l=0, l \neq j}^k \frac{\xi - \lambda x_{GL}^l}{\lambda x_{GL}^j - \lambda x_{GL}^l} \right) \\ &= \frac{1}{\lambda^k} \prod_{l=0, l \neq i}^k \frac{\xi - \lambda x_{GL}^l}{x_{GL}^i - x_{GL}^l} \end{aligned}$$

Remark:

$$\begin{aligned}
& \left(\int_0^\lambda \alpha_*(\xi_0 + \xi) \varphi_j(\xi) \varphi_i(\xi) d\xi \right)_{0 \leq i, j \leq k} \\
&=_{\alpha_* = \alpha = cte} \left(\frac{\alpha}{\lambda^{2k}} \int_0^\lambda \left[\prod_{l=0, l \neq i}^k \frac{\xi - \lambda x_{\text{GL}}^l}{x_{\text{GL}}^i - x_{\text{GL}}^l} \prod_{l=0, l \neq i}^k \frac{\xi - \lambda x_{\text{GL}}^l}{x_{\text{GL}}^j - x_{\text{GL}}^l} \right] d\xi \right)_{0 \leq i, j \leq k} \\
&=_{\substack{\xi = \lambda \xi' \\ d\xi = \lambda d\xi'}} \left(\frac{\alpha}{\lambda^{2k}} \int_0^1 \left[\prod_{l=0, l \neq i}^k \frac{\lambda \xi' - \lambda x_{\text{GL}}^l}{x_{\text{GL}}^i - x_{\text{GL}}^l} \prod_{l=0, l \neq i}^k \frac{\lambda \xi' - \lambda x_{\text{GL}}^l}{x_{\text{GL}}^j - x_{\text{GL}}^l} \right] \lambda d\xi' \right)_{0 \leq i, j \leq k} \\
&= \left(\frac{\alpha}{\lambda^{2k}} \int_0^1 \left[\prod_{l=0, l \neq i}^k \lambda \frac{\xi' - x_{\text{GL}}^l}{x_{\text{GL}}^i - x_{\text{GL}}^l} \prod_{l=0, l \neq i}^k \lambda \frac{\xi' - x_{\text{GL}}^l}{x_{\text{GL}}^j - x_{\text{GL}}^l} \right] \lambda d\xi' \right)_{0 \leq i, j \leq k} \\
&= \left(\alpha \lambda \int_0^1 \left[\prod_{l=0, l \neq i}^k \frac{\xi' - x_{\text{GL}}^l}{x_{\text{GL}}^i - x_{\text{GL}}^l} \prod_{l=0, l \neq i}^k \frac{\xi' - x_{\text{GL}}^l}{x_{\text{GL}}^j - x_{\text{GL}}^l} \right] d\xi' \right)_{0 \leq i, j \leq k} \\
&= \alpha \lambda \left(\int_0^1 \tilde{\varphi}_j(\xi) \tilde{\varphi}_i(\xi) d\xi \right)_{0 \leq i, j \leq k}
\end{aligned} \tag{15}$$

with $\tilde{\varphi}_i$ the polynomials for a unit element $[\xi_0, \xi_0 + 1]$

Et par exemple pour $k = 1$, $\varphi_1(\xi) = \frac{\lambda - \xi}{\lambda}$, $\varphi_2(\xi) = \frac{\xi}{\lambda}$.

Pour le cas particulier où $\alpha = cte$, l'intégrale (14) revient à intégrer un polynôme de degrés $2k$. En évaluant celle-ci par $k + 2$ points de GL (car exacte à $2n - 3$), on obtient l'intégrale exacte.

Nous allons construire également le second membre SMB qui provient des termes de bord inhomogènes:

$$SMB_i = \int_{\partial\Omega} b(x, y) \Phi_i(x, y).$$

Ce terme est non trivialement nul si le sommet i appartient à $\partial\Omega = \Gamma_b \cup \Gamma_t \cup \Gamma_l \cup \Gamma_r$. Pour un élément de référence de la forme $[\xi_0, \xi_0 + \delta]$, le vecteur élémentaire associé à ce terme inhomogène est de la forme

$$vecb = \left(\int_0^\lambda b_*(\xi_0 + \xi) \varphi_i(\xi) d\xi \right)_{1 \leq i \leq k+1},$$

avec $\varphi_1(\xi) = \frac{\delta - \xi}{\delta}$, $\varphi_2(\xi) = \frac{\xi}{\delta}$ et $\beta_*(\xi_0 + \xi)$ coïncide avec $\beta_*(\xi_0 + \xi) = \beta(V_0|_x + \xi t_x, V_0|_y + \xi t_y)$ et \vec{t} est le vecteur unitaire orienté de V_0 à V_1 . Également, cette intégrale pourra être intégrée par GL.

3.4 Numerical Validation

In this section, we check the validity of our model. Thus, we compare our model with a manufactured analytical solution (see appendix A). We there-

fore consider the [Helmholtz \(1868\)](#) equation with mixed Dirichlet and Robin boundary conditions, below equation (16).

$$\begin{cases} \Delta u + k^2 u = f(x, y) & , \quad \text{in } \Omega, \\ u = u_{\text{exact}} & , \quad \text{on } \Gamma_2 \cup \Gamma_3 \cup \Gamma_4, \\ \frac{\partial u}{\partial n} + i k u = g(x, y) & , \quad \text{on } \Gamma_1, \end{cases} \quad \begin{array}{c} \Gamma_3 \\ \square \\ \Omega \\ \Gamma_4 \\ \Gamma_2 \\ \Gamma_1 \end{array} \quad (16)$$

For this analytical case, we take the geometry of a unit square and link it with regular triangles, irregular triangles, irregular quadrilaterals and polygons. To generate these meshes, we use the Gmsh ([Geuzaine et al. 2009](#)) and PyPoly-Mesher ([Talischi et al. 2012](#)). We perform calculations from order 1 to order 5 on maximum cell diameters h from 0.05 to 0.7 m. We then compute the L^2 error for each calculation. The results are shown in figure 4.

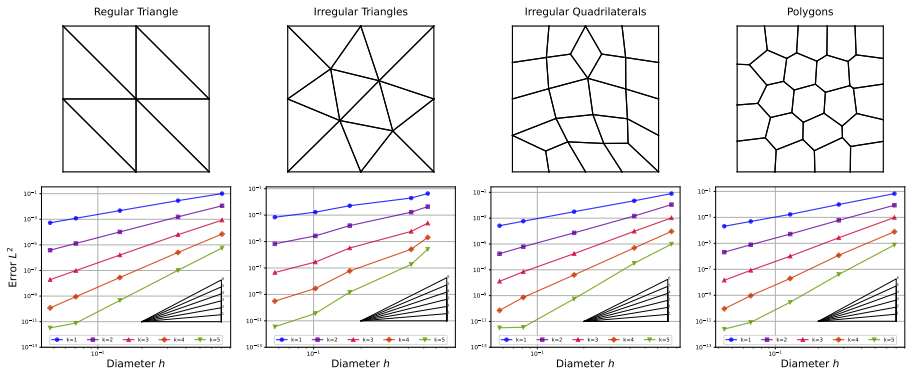


Figure 4: Convergence of order $\mathcal{O}(h^{k+1})$.

We find the expected superconvergence of order $\mathcal{O}(h^{k+1})$.

Remarks: For a validation with the Mild-Slope equation, the order would have been less good, given the approximation we have made per cell.

4 Numerical Application

On prend un truc bidon sur un port ou qqc du genre

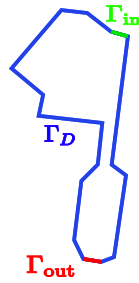
4.1 Sensibilité de la pente, Helmholtz vs Berkhoff

On introduit un déferlement selon ([Munk 1949](#)) Problem conditions:

- $a_{\max} = 2$ m,



Port location



Port boundary

The Helmholtz or **Mild-Slope** equation:

$$\left\{ \begin{array}{ll} \nabla(\mathbf{C}_p \mathbf{C}_g \nabla a) + k^2 \mathbf{C}_p \mathbf{C}_g a = 0, & \text{in } \Omega, \\ a = 0, & \text{in } \Gamma_{\text{in}}, \\ \frac{\partial a}{\partial n} + ik a = 0, & \text{in } \Gamma_{\text{out}}, \\ a = \gamma a_i & \text{in } \Gamma_D. \end{array} \right.$$

- $T_0 = 8$ s,
- $\theta = 280^\circ$.

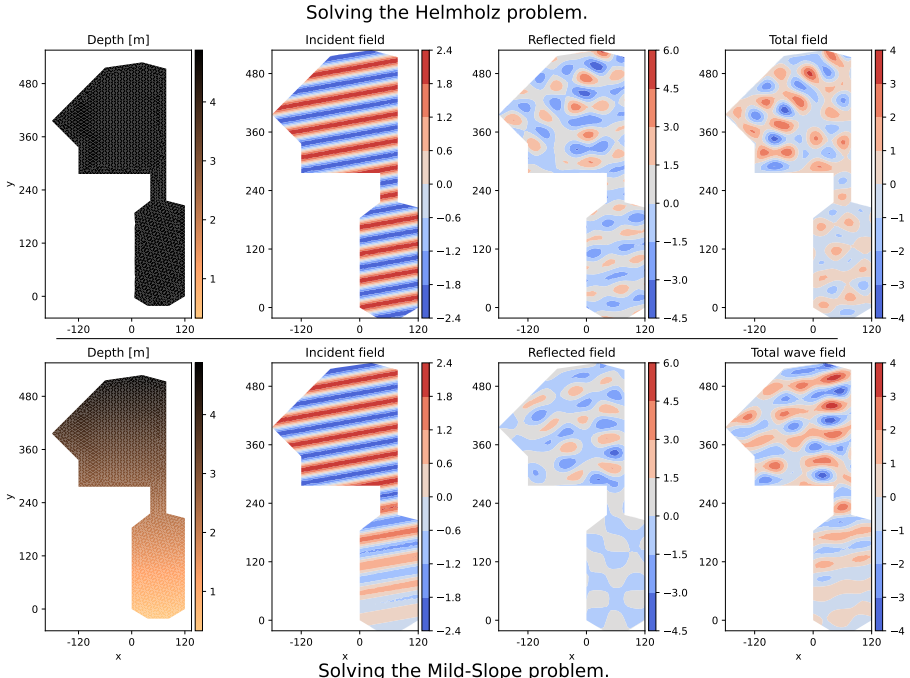


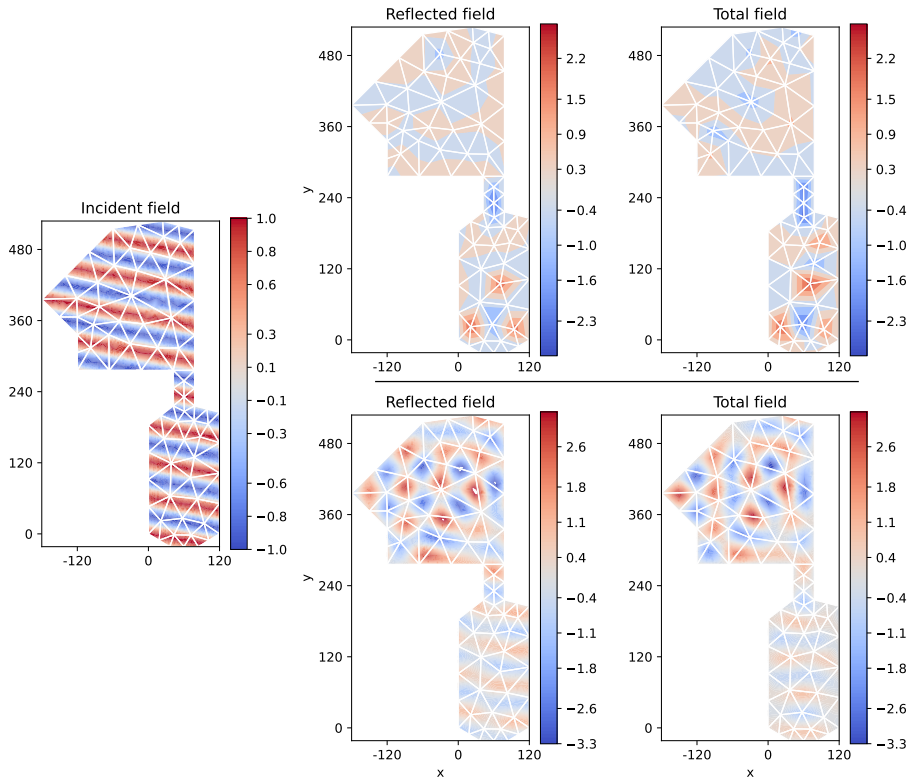
Figure 5: Caption

4.2 Application claquée - Résultats avec différents k

Problem conditions:

- $a_{\max} = 1 \text{ m}$,
- $T_0 = 8 \text{ s}$,
- $\theta = 250^\circ$.

Solving the Helmholtz problem with $k=1$



Solving the Helmholtz problem with $k=5$

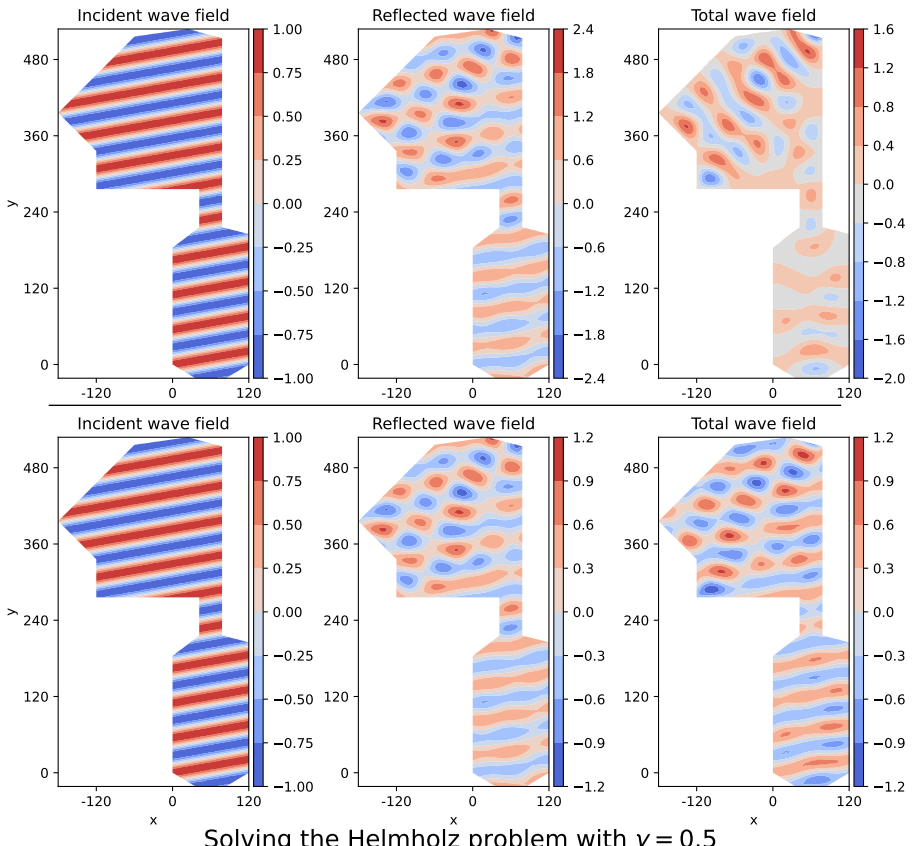
Figure 6: Caption

4.3 Sensibilité du coefficient de réflexion

Problem conditions:

- $a_{\max} = 1 \text{ m}$,
- $T_0 = 8 \text{ s}$,
- $\theta = 280^\circ$.

Solving the Helmholtz problem with $\gamma = 1$



Solving the Helmholtz problem with $\gamma = 0.5$

Figure 7: Caption

4.4 Appli montrant intérêt Robin

$$\begin{cases} \Delta u + k^2 u = 0 & , \text{ in } \Omega , \\ u = -u_{\text{inc}} & , \text{ on } \Gamma_D , \\ \frac{\partial u}{\partial n} + i k u = 0 & , \text{ on } \Gamma_{\text{Inf}} . \end{cases}$$

or

$$\begin{cases} \Delta u + k^2 u = 0 & , \text{ in } \Omega , \\ u = -u_{\text{inc}} & , \text{ on } \Gamma_D , \\ \frac{\partial u}{\partial n} = 0 & , \text{ on } \Gamma_{\text{Inf}} . \end{cases}$$

- $a_{\max} = 1 \text{ m}$,

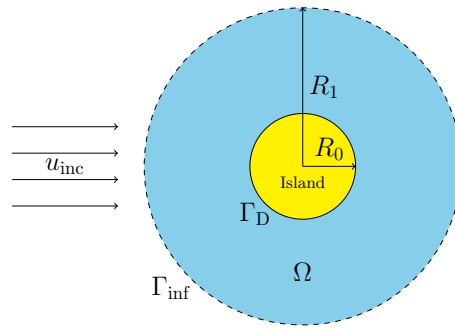
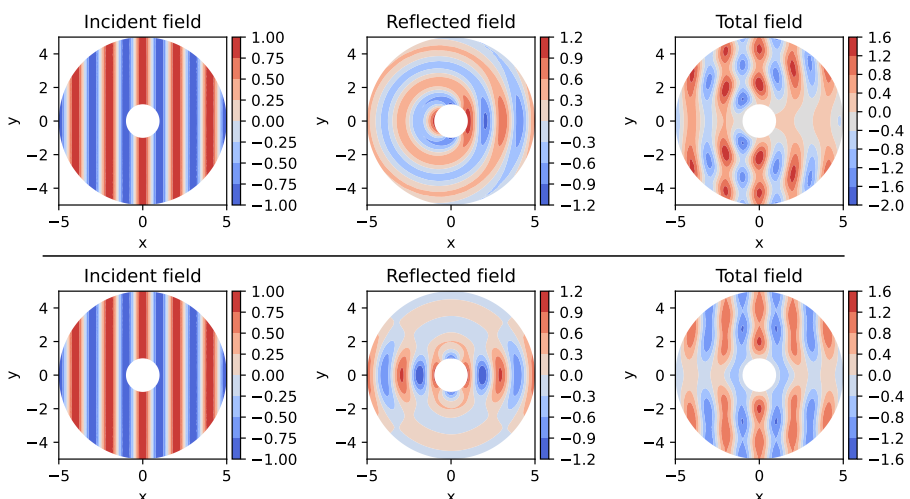


Figure 8: Caption

- $T_0 = 20$ s,
- $\theta = 0^\circ$.

Solving the Helmholtz problem with a Robin condition on Γ_{inf}



Solving the Helmholtz problem with a Neuman condition on Γ_{inf}

Figure 9: Caption

5 Conclusion and Discussion

On est content

6 Declarations

6.1 Availability of data and material

All data, models, and code generated or used during the study are available on request.

6.2 Conflict of interest

The authors declare that they have no conflict of interest.

6.3 Acknowledgements

This work was conducted as part as M. Dupont's PhD studies which is funded by the CNRS with the MITI grant. We gratefully acknowledge funding from CNRS, OPTIBEACH projects and FEDER Europe.

Appendix

A Manufactured analytical solution

The solution to the equation 16 problem has been produced using the following functions:

$$\begin{aligned} u_{\text{exact}}(x, y) &= (x + y) \cdot (1 + i) + \exp(x^2 + iy^2), \\ f(x, y) &= -((2x)^2 + (2iy)^2 + 2(1+i)) \cdot \exp(x^2 + iy^2) + k^2 \cdot u_{\text{exact}}(x, y), \\ g(x, y) &= (1+i) + (2iy) \cdot \exp(x^2 + iy^2) + ik \cdot u_{\text{exact}}(x, y). \end{aligned} \tag{A1}$$

This produces the complex analytical solution that can be seen below in figure A1.

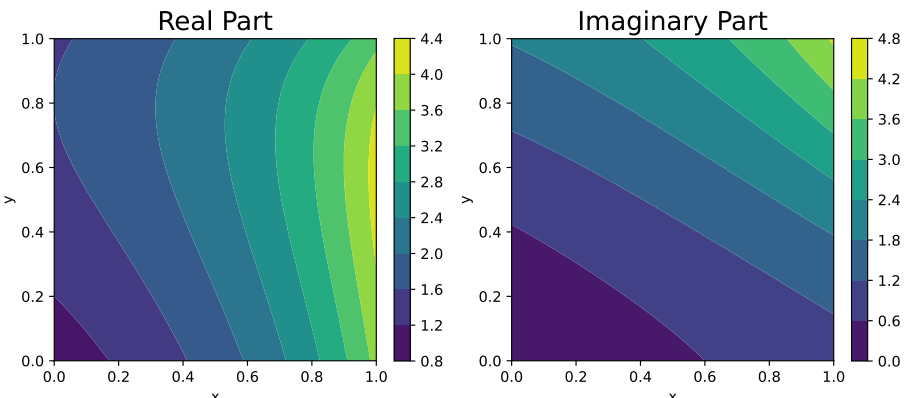


Figure A1: Real and Imaginary part of u_{exact} .

References

- Airy, George Biddell (1845). *Tides and waves*. B. Fellowes.
- Beirão da Veiga, L., F. Brezzi, L. D. Marini, and A. Russo (2014). “The Hitch-hiker’s Guide to the Virtual Element Method”. In: *Mathematical Models and Methods in Applied Sciences* 24.08, pp. 1541–1573. DOI: [10.1142/S021820251440003X](https://doi.org/10.1142/S021820251440003X).
- Berkhoff, J.C.W. (1972). “COMPUTATION OF COMBINED REFRACTION - DIFFRACTION”. In: *Coastal Engineering Proceedings* 1.13, p. 23. DOI: [10.9753/icce.v13.23](https://doi.org/10.9753/icce.v13.23).
- Booij, N. (1983). “A note on the accuracy of the mild-slope equation”. In: *Coastal Engineering* 7.3, pp. 191–203. DOI: [https://doi.org/10.1016/0378-3839\(83\)90017-0](https://doi.org/10.1016/0378-3839(83)90017-0).
- Geuzaine, Christophe and Jean-François Remacle (2009). “Gmsh: A 3-D finite element mesh generator with built-in pre-and post-processing facilities”. In: *International journal for numerical methods in engineering* 79.11, pp. 1309–1331.
- Guo, Junke (2002). “Simple and explicit solution of wave dispersion equation”. In: *Coastal Engineering* 45.2, pp. 71–74. DOI: [https://doi.org/10.1016/S0378-3839\(02\)00039-X](https://doi.org/10.1016/S0378-3839(02)00039-X).
- Helmholtz, Professor (1868). “XLIII. On discontinuous movements of fluids”. In: *The London, Edinburgh, and Dublin Philosophical Magazine and Journal of Science* 36.244, pp. 337–346.
- Mascotto, Lorenzo, Ilaria Perugia, and Alexander Pichler (2019). “A nonconforming Trefftz virtual element method for the Helmholtz problem”. In: *Mathematical Models and Methods in Applied Sciences* 29.09, pp. 1619–1656. DOI: [10.1142/S0218202519500301](https://doi.org/10.1142/S0218202519500301).
- Munk, Walter (1949). “The solitary wave theory and its application to surf problems”. In: *Annals of the New York Academy of Sciences* 51, pp. 376–424. DOI: [10.1111/j.1749-6632.1949.tb27281.x](https://doi.org/10.1111/j.1749-6632.1949.tb27281.x).
- Perugia, Ilaria, Paola Pietra, and Alessandro Russo (2016). “A plane wave virtual element method for the Helmholtz problem”. In: *ESAIM: Mathematical Modelling and Numerical Analysis* 50.3, pp. 783–808. DOI: [10.1051/m2an/2015066](https://doi.org/10.1051/m2an/2015066).
- Talischi, Cameron, Glauco H Paulino, Anderson Pereira, and Ivan FM Menezes (2012). “PolyMesher: a general-purpose mesh generator for polygonal elements written in Matlab”. In: *Structural and Multidisciplinary Optimization* 45, pp. 309–328.